The melting of poly (ι-lactic acid)

Abdul Aziz, Azizan; Hay, James; Jenkins, Michael

DOI:
10.1016/j.eurpolymj.2018.01.041

Document Version
Peer reviewed version

Citation for published version (Harvard):
Abdul Aziz, A, Hay, J & Jenkins, M 2018, 'The melting of poly (ι-lactic acid)', *European Polymer Journal*, vol. 100, pp. 253-257. https://doi.org/10.1016/j.eurpolymj.2018.01.041

The melting of Poly (L-lactic acid).

by

Azizan A Aziz, James N. Hay* and Michael J. Jenkins,

The School of Metallurgy and Materials,

College of Engineering and Physical Science,

University of Birmingham,

Edgbaston,

Birmingham B15 2TT, UK

Figures: - 11.

Tables: - 1.

*Corresponding Author

Tel: +44 121 414 4544 Fax: +44 121 414 5232

E-mail address: j.n.hay@bham.ac.uk.

The melting of Poly (lactic acid).

by

Azizan A Aziz, James N. Hay* and Michael J. Jenkins,

The School of Metallurgy and Materials, College of Engineering and Physical Science,

University of Birmingham, Edgbaston, Birmingham B15 2TT, UK.

Abstract.

The effect of crystallization temperature and time on the melting of a stereo-copolymer of L-lactic acid has been measured using differential scanning calorimetry and hot stage microscopy. The temperature of the last trace of crystallinity increased with time and temperature. Increasing the heating rate to 50 ^{o}C min^{-1} and correcting for thermal lag enabled the m.pt of the as-crystallized material to be determined without premature melting and recrystallization of the sample on heating. The measured melting points enabled the equilibrium m.pt. of the copolymer to be determined as 205 ±2 ^{o}C.

Changes due to lamellae thickening occurred by secondary crystallization from the initial onset of crystallization increasing with increasing temperature consistent with the process being diffusion controlled. The addition of small chain segments emerging from the top lamellar surface occurred by reptation and growth increased with the square root of the elapsed time. This is consistent with the process of secondary crystallization.

Keywords: Melting

Stem lengths

Diffusion control

Secondary Crystallization.

1.0 Introduction

The melting of polymers is different from that of low molar mass materials in that melting generally occurs over a wider temperature range and is dependent on thermal history [1]. The presence of multiple melting endotherms is common and has been observed with many semi-crystalline polymers, copolymers and blends [1-4]. A variety of effects have been invoked to explain the phenomenon, to the presence of more than one crystallographic form (polymorphism) [5], to the presence of melting/re-crystallisation and re-melting [6]; to changes in morphology [7], to lamellar thickening and crystal perfecting [8,9], to changes in orientation[10] and to the effect of molecular weight distribution [11]. It is more than likely that one of these mechanisms alone cannot explain the observation of multiple endotherms.

The stereo-copolymer of lactic acid, sco-PLA, because of its low crystallization rates can readily be crystallised to different degrees of crystallinity over a wide temperature range and for different times. Since samples crystallised at different temperatures to the same degree of crystallinity have different melting behaviour [1] this makes it particularly suited to test the various mechanisms which have been suggested to account for the dependence of the observed melting points on experimental conditions.

Sco-PLA was crystallized isothermally for various periods and over a wide temperature range, 95 to 135 ^{o}C and heated directly to the melting point at different heating rates, from 10 to 50 ^{o}C min^{-1} to determine effect on the shape of the melting endotherms and the melting point defined as the temperature corresponding to the last final of crystallinity used to determine the equilibrium melting point, T^{o}_{m}, and calculate the thickness of the lamellae.

2.0 Experimental

The material used in this study was a random copolymer of stereoisomers of L-lactic acid with 4% D-lactic acid and a molecular weight of 194 kg mol^{-1}. It was supplied in pellet form, PLA20002D, by NatureWorks LLC, Minnetonka, MN, USA as a semi-crystalline co-polymer.

A Perkin-Elmer differential scanning calorimeter, model DSC 7, interfaced to a PC and controlled by Pyris software, was used to characterise the thermal properties of the copolymer. The block of the calorimeter was connected to a Grant Intracooler to control the temperature of the DSC down to 5 ^{o}C and enabled the calorimeter to be cooled to room temperature while maintaining cooling at 50 ^{o}C min^{-1}. The temperature and thermal response of the calorimeter was calibrated from the melting points and the enthalpy of fusion of ultra-pure metals; indium (m. pt. 156.63 ^{o}C, Δh_f 29.2 Jg^{-1}), tin (m. pt. 231.91 ^{o}C) and lead (m. pt. 327.50 ^{o}C). An "empty pan" baseline was established for the calorimeter using two empty aluminium DSC pans of equal mass and subtracted from the heat flow-temperature response of the sample.

Samples of the 'as received' PLA were weighed and sealed into a DSC aluminium pan with lid. Most were 6.0± 0.1mg except for the samples used to determine thermal lag which varied from 2-12 mg. In order to remove thermal history and produce an amorphous sample, it was heated from 30 to 200 °C at a heating rate of 10 °C min^{-1}, held in the melt for 2 minutes at 200 °C before being cooled at 50 ^{o}C min^{-1} to room temperature. This sample exhibited no melting endotherm on subsequent heating to the m.pt.

Prior to studying melting behaviour samples were heated to 200 ^{o}C, held for 2 min and cooled at 50 ^{o}C min^{-1} to the crystallization temperature, 95 to 135 ^{o}C. They were subsequently crystallized for 2-16 h and melted at 50 ^{o}C min^{-1}. Corrections were made for

the thermal lag at this heating rate by extrapolation to zero weight. The fractional crystallinity developed was determined from the heat of fusion, ΔH_t, since

$$X_t = \Delta h_t / \Delta h^o_f \qquad (1).$$

where Δh^o_f is the heat of fusion of crystalline PLA, taken to be 93.6 Jg^{-1} [12]. The m.pt, T_m, was defined by the temperature corresponding to the last trace of crystallinity.

A Leitz Dialux-Pol polarising light binocular microscope with long distance working object lenses, x10, x32 and x50 magnification, and x10 eye-piece lens was used to measure the crystallization of thin films, 10-15μm thick. The films were held horizontally in a hot stage, Linkam THM 600 equipped with a thermal control unit. Digital and video cameras, charge-coupled devices (CCD), enabled images to be captured with time and measured directly on the computer screen. The effect of crystallization temperature on spherulite growth rate and nucleation density was measured over the range 95-135 ^oC.

3.0 Results and Discussion.

3.1. Spherulitic Crystallization.

PLA produced regular spherulites with distinct Maltese cross under polarised light, see Fig. 1. Heterogeneous nucleation of the spherulites was observed since their number in the field of view did not increase with time. However the nucleation density, N, increased markedly with decreasing crystallization temperature; see Fig 2, in keeping with the decrease in the critical size of the nucleus and a dependence on the undercooling from the m.pt, ΔT, [13],

$$N = N_o \exp (-K T^o_m / \Delta T f) \qquad (2)$$

Where N_o is a pre-exponential factor, K is the growth nucleation parameter, T^o_m the equilibrium m.pt. is 205 ^oC, and $\Delta T = (T^o_m - T)$ is the degree of supercooling. The correction factor for the temperature dependence of heat of fusion is $f = 2T/ (T^o_m + T)$.

The plot of ln (N) against $T^{o}_{m}/\Delta T$ f was linear, see Fig 3, from which the heterogeneous nucleation constant, K, was 950 ± 50 K^{-1} .

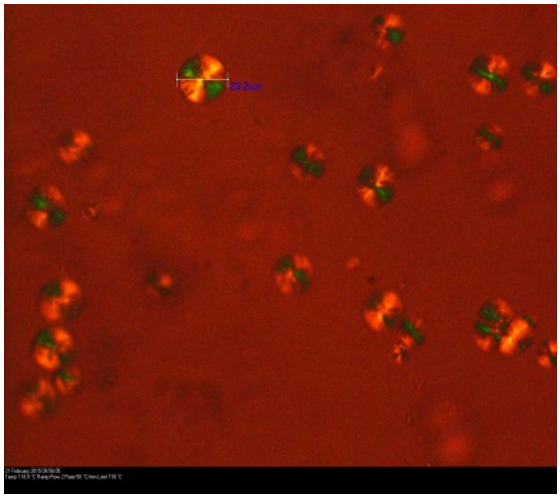

a. 900 min

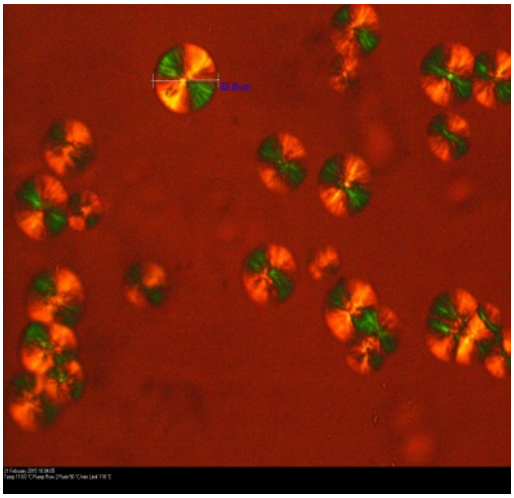

b. 1000 min

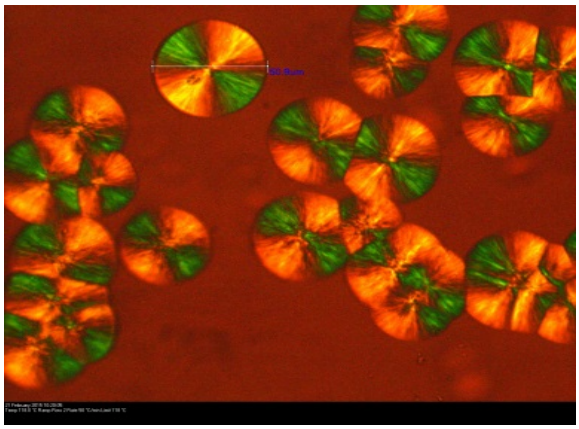

c. 1100 min

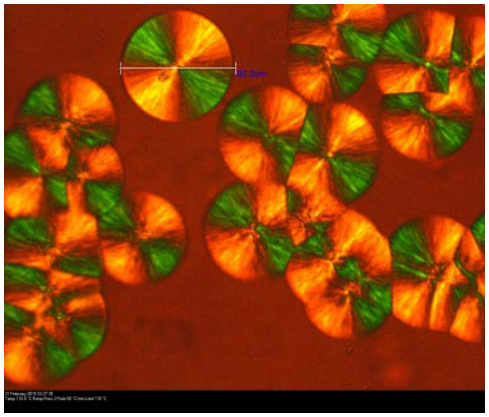

d. 1500 min

Fig. 1. Development of spherulites with time at 118 ^{o}C.

The spherulite radius increased linearly with time up to impingement with neighbouring spherulites and the radial growth rate, g = dr/dt exhibited a bell-shaped dependence on crystallization temperature with a maximum at 126 ^{o}C. This dependence of growth rate on temperature is attributed to two effects, namely diffusion of chain segments at low temperature as the glass transition is approached and nucleation control at temperatures close to the m.pt.

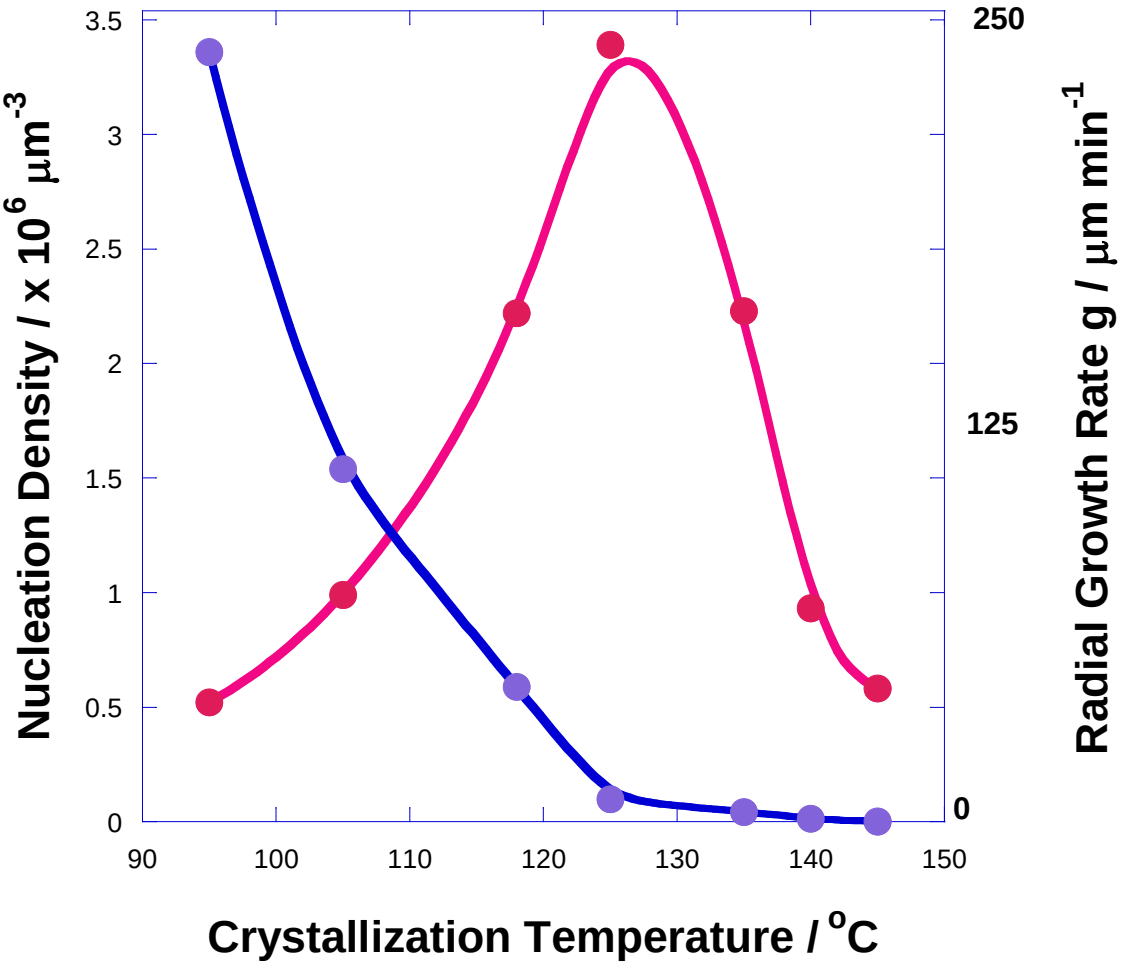

Fig. 2. Dependence of Radial Growth Rate and Nucleation Density on Crystallization Temperature.

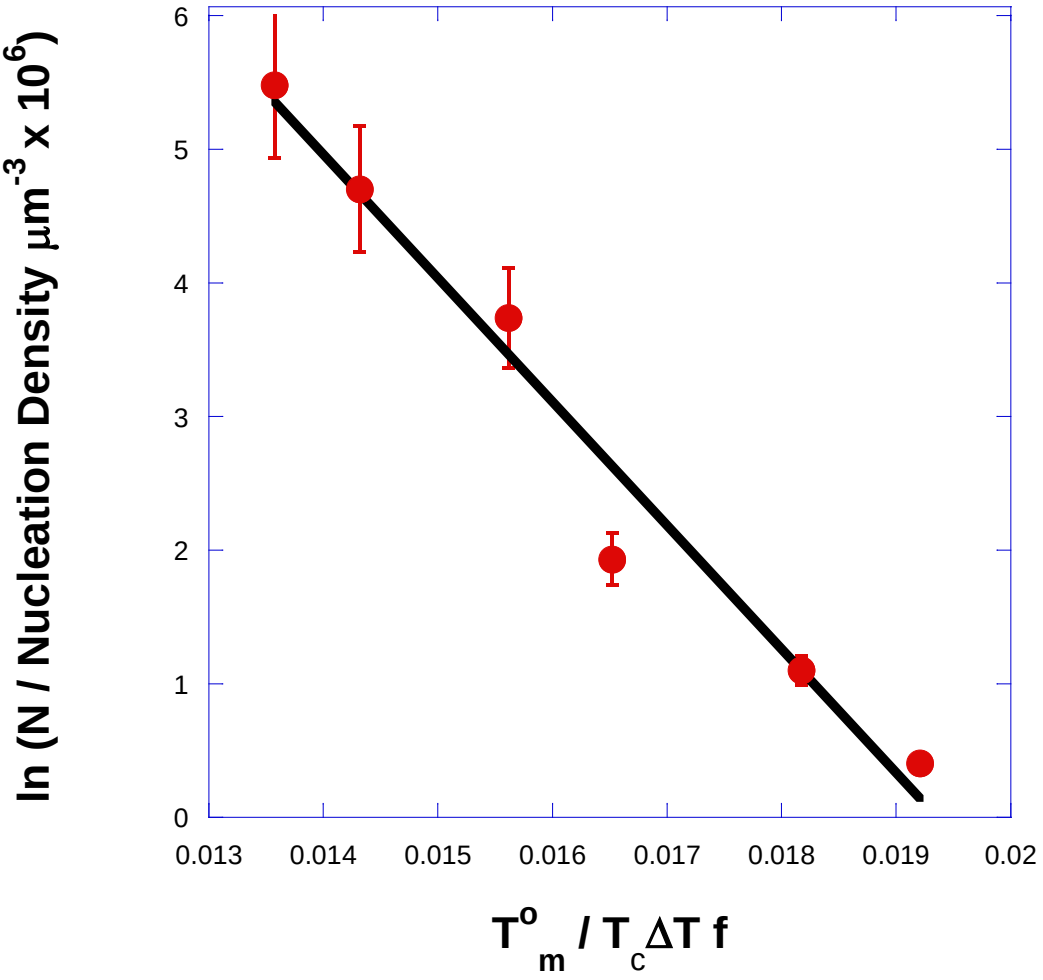

Fig. 3. Dependence of Nucleation Density on degree of Supercooling.

Hoffman and colleagues [13] derived a theoretical expression for the temperature dependence of the growth rate incorporating a term for chain transport to account for crystallization ceasing at the onset of the glass transition and also nucleation control of lamellar growth close to the m.pt, i.e.

$$\ln (g) = \ln (g_o) - U/R\,(T-T_2) - K_g T^o_m / (T\Delta Tf) \qquad (3)$$

Where g_o is a pre-exponential factor, U is activation energy for transport of chain segments to the crystal growth face, T_2 is the thermodynamic glass transition temperature, and K_g is the growth nucleation parameter.

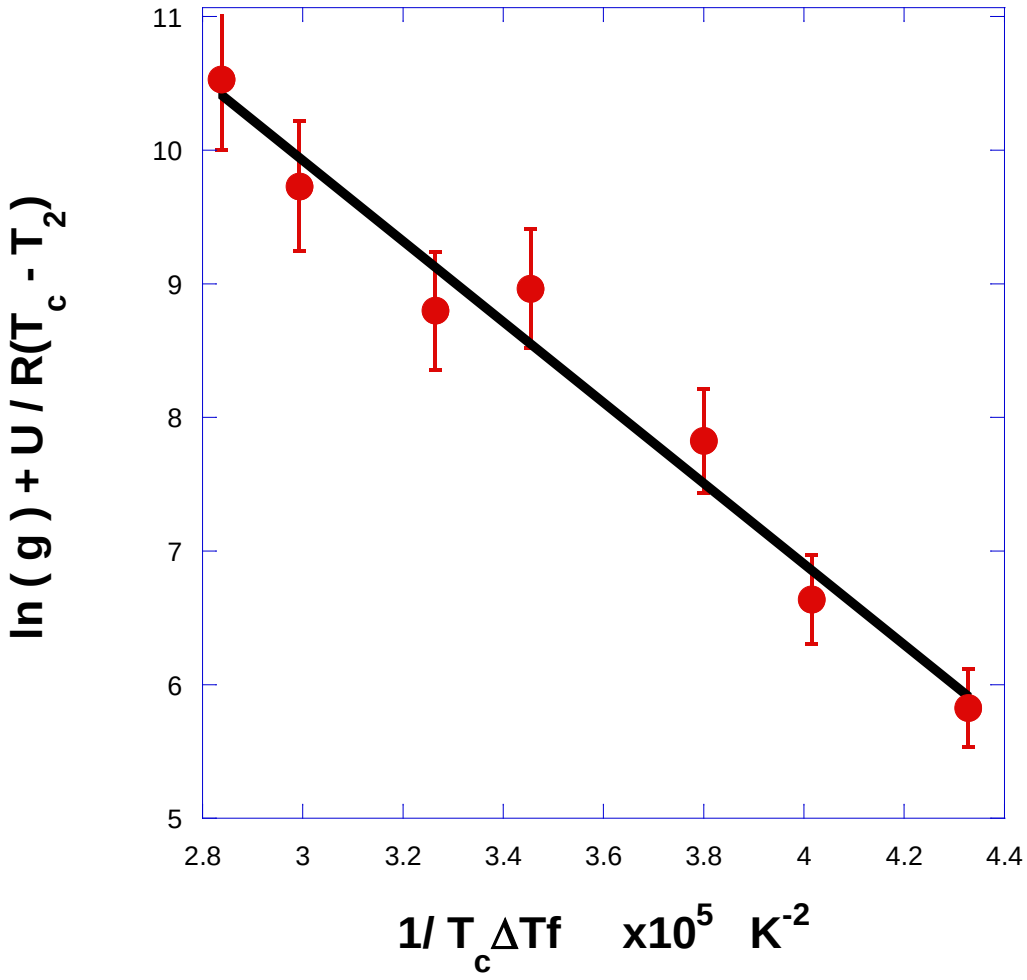

Fig. 4. Dependence of growth rate on degree of supercooling.

From the plot of ln(g) $+U/R(T_c-T_2)$ against $1/T_c\Delta Tf$, see Fig. 4, the nucleation constant was $3.02\pm 0.50 \times 10^5$ K^2 and since this covers to a very high degree of supercooling, 60 to 120 ^oC, nucleation must occur in regime ll. Accordingly

$$K_{ll} = 4b\sigma\sigma_e T^o_m / k\Delta h_v \quad (4)$$

Where b is the monomolecular layer thickness, $5.2x10^{-10}$ m, σ and σ_e the lateral and fold surfaces free energies, T^o_m the equilibrium melting point, k Boltzmann constant, $1.38x10^{-23}$ J K^{-1}, Δh_v, the enthalpy of fusion per unit volume, $111.1 x10^{6}$ J m^{-3}. Taking $\sigma = 12.0x10^{-3}$ Jm^{-2}, [12] and $\sigma.\sigma_e = 468 \times 10^{-6}$ J^2m^{-4} σ_e is accordingly $39 \pm 6 x10^{-3}$ Jm^{-2}

This value is substantially lower than that for PLLA, $61 x10^{-3}$ J m^{-2}, and must be attributed to rejection of the D-isomer from the crystalline regions due to its disruptive effect on the packing of the L segments emerging from the fold surface.

3.2 Melting Studies.

PLA was slow to crystalize and direct measurement of the crystallization rate with time by DSC was severely limited even at the fastest rate at 105 ^oC which took 210 min, see Fig.5, to reach 0.30 fractional crystallinity. The development of crystallinity with time was measured from the heat of fusion from the heating curve at 50 ^oC min^{-1} observed after leaving the sample for 2, 4, 6 and 16 h. at each temperature in the range 85-135 ^oC. The minimum in crystallization time, at about 105 ^oC, is a combination of the increase in nucleation density with decreasing temperature and a maximum in growth rate at 125 ^oC as observed previously.

The melting endotherms, see Fig. 6, exhibited a single distribution and there was no evidence of multiple melting points as observed on heating at slower rates and attributed to annealing the sample on heating to the m.pt.. The endotherms were displaced to higher temperatures with time and at higher crystallization temperature as can be seen in Fig. 7 where the temperature at the last trace of crystallinity, T_m, is plotted against crystallization time at each crystallization temperature.

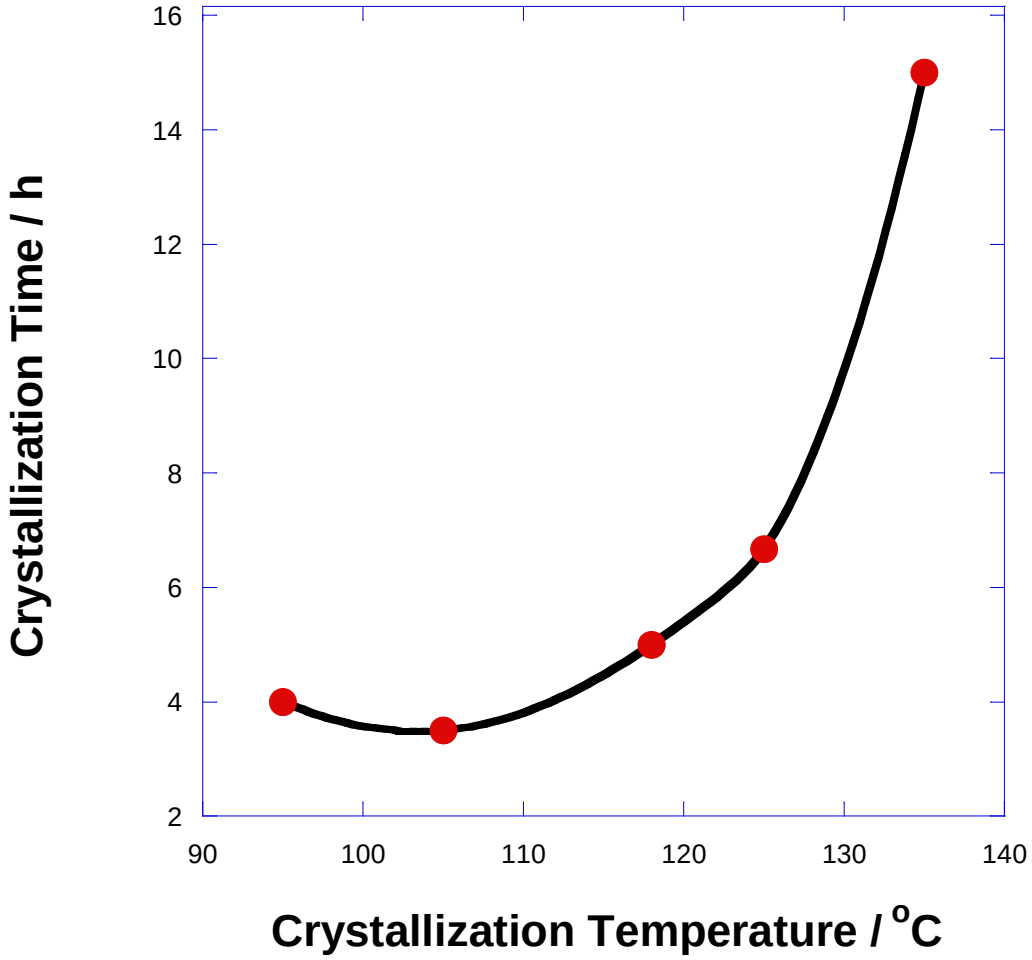

Fig 5. Effect of crystallization temperature on the time to reach 0.30 fractional crystallinity.

The m. pts. at constant crystallization temperature increased with time from the beginning of the crystallization, consistent with lamellae thickening occurring from the time the lamellae initially formed implying that secondary crystallization coexisted with primary from the early stages of crystallization and that the observed samples all have some degree of thickening. To eliminate this values of T_m were extrapolated to zero time, see Fig.7.

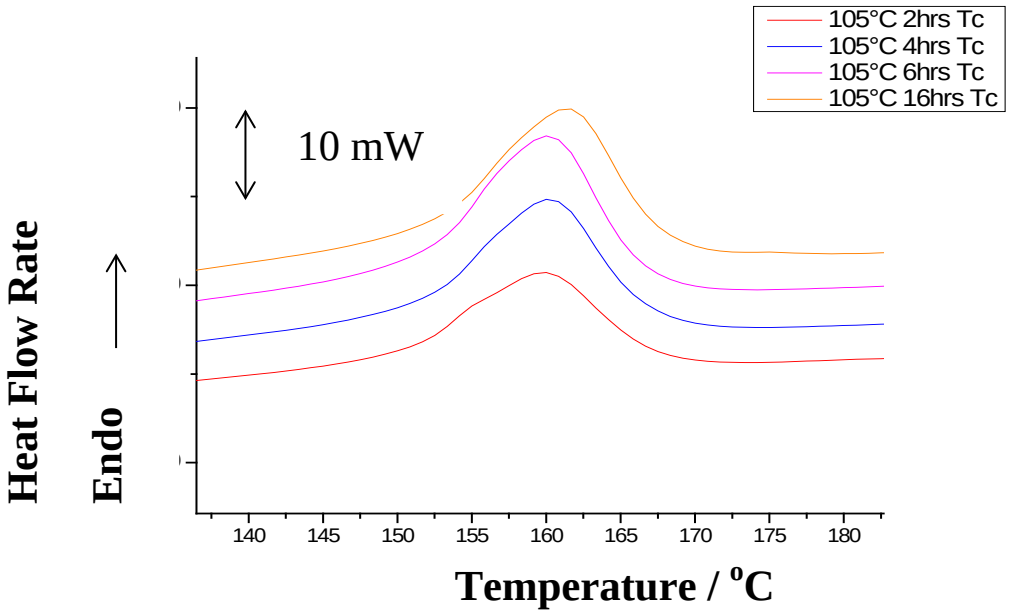

Crystallized at 105 °C.

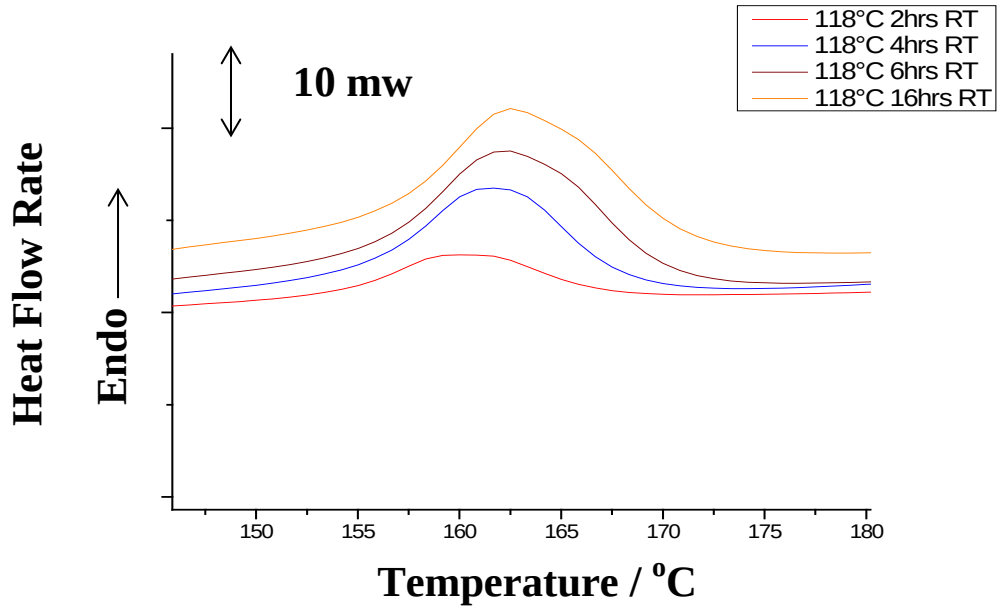

Crystallized at 118 °C.

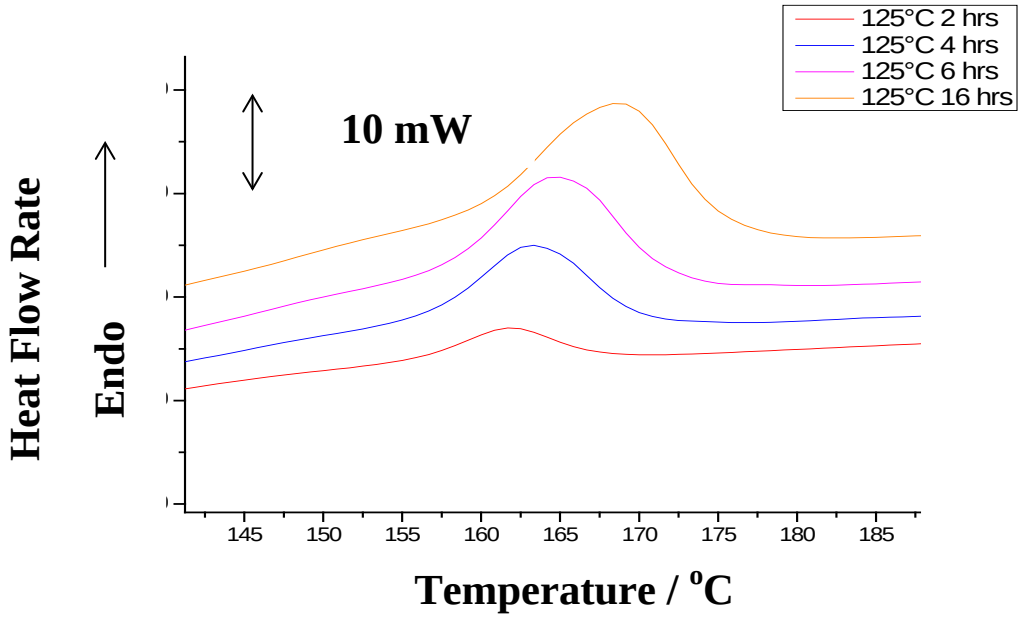

Crystallized at 125 °C

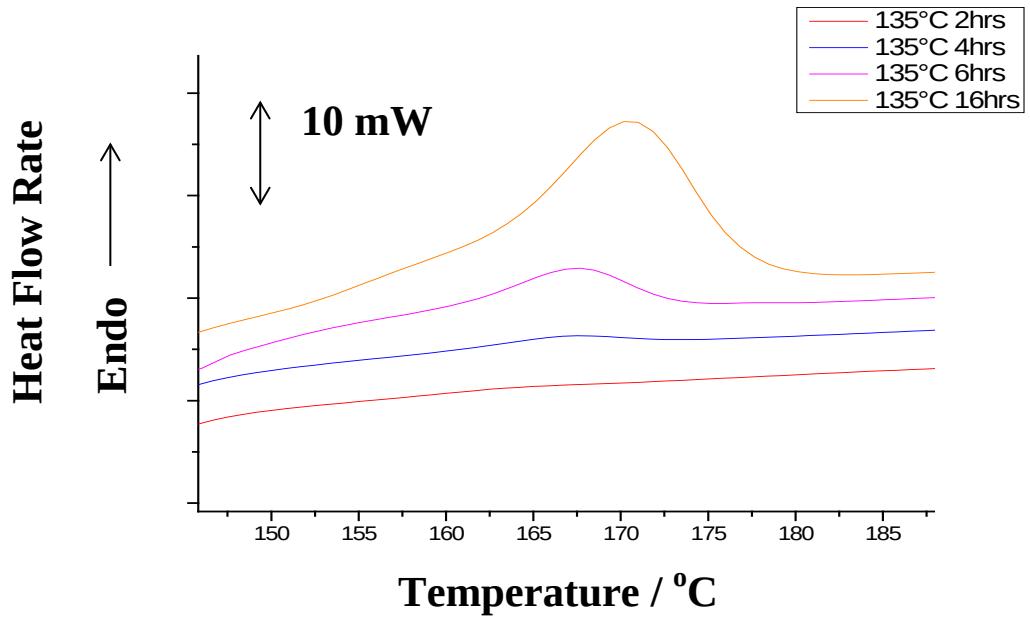

Crystallized at 135 °C

Figure 6. Melting endotherms produced after crystallizing at each temperature for 2, 4, 6 and 16 h.

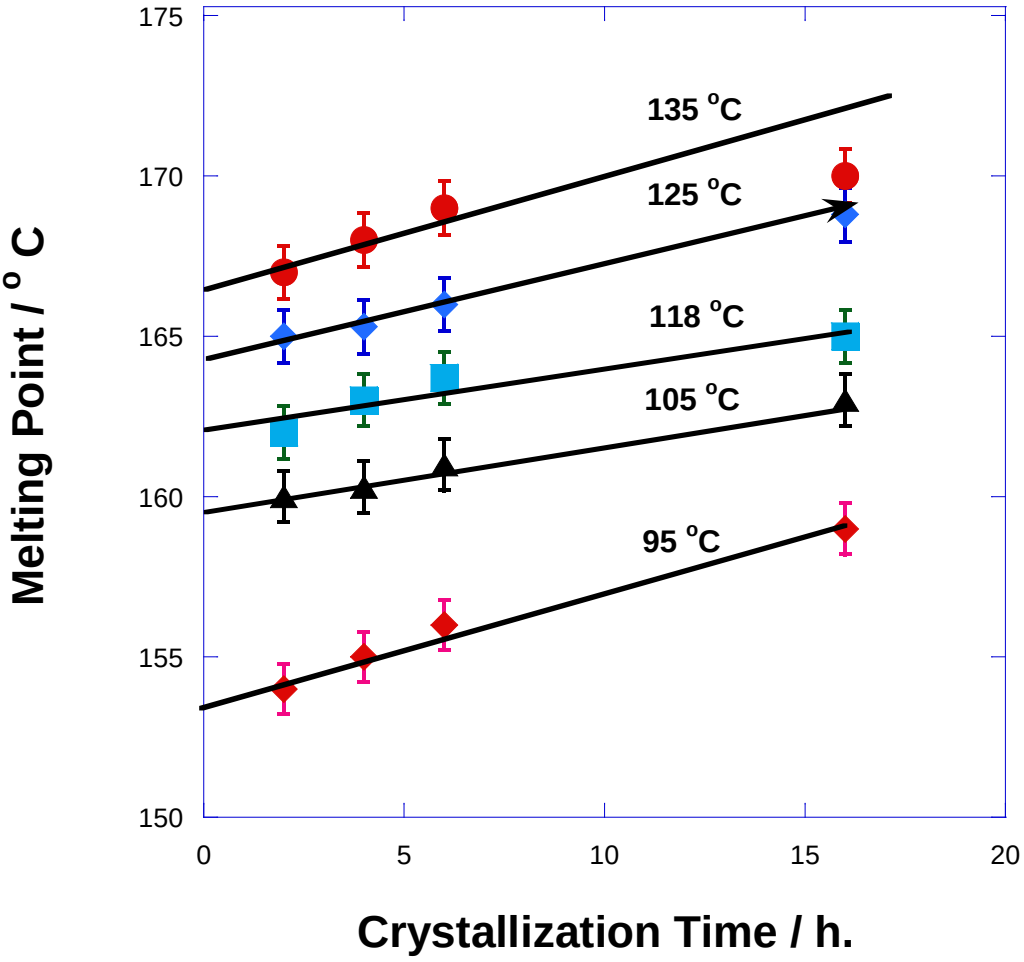

Fig. 7. Increase in m.pt with crystallization time and temperature.

The extrapolated values increased with crystallization temperature in line with Hoffman and Weeks' nucleation theory of crystal growth [14] relating T_m measured under equilibrium conditions to the crystallization temperature, T_c. Adopting the form of the equation used by Pennings et al. [15]

$$T_m = T^o_m (1- 1/2\beta) + T_c/2\beta \qquad (5).$$

Where $\beta = (\sigma_e \xi / \sigma \xi_e) = 1.0$ in absence of annealing of the sample on heating to the m.pt. at 50 ^oC min^{-1}.

With σ and σ_e the surface free energy of the fold surface measured at the crystallization and melting temperature.. Similarly ξ_e and ξ is the lamellae thickness under these conditions. A linear plot of T_m *vs.* T_c was observed, see Fig.8, from which the value of the lamella thickening coefficient, β, was 1.0 indicating that annealing or crystal perfecting had not occurred substantially. This compares with values of 1.2 – 1.4 observed for PLLA on measuring the m.pts at lower heating rates. The extrapolated value of T^o_m was 205 ± 2 ^oC in good agreement with literature values for PLLA [12, 15].

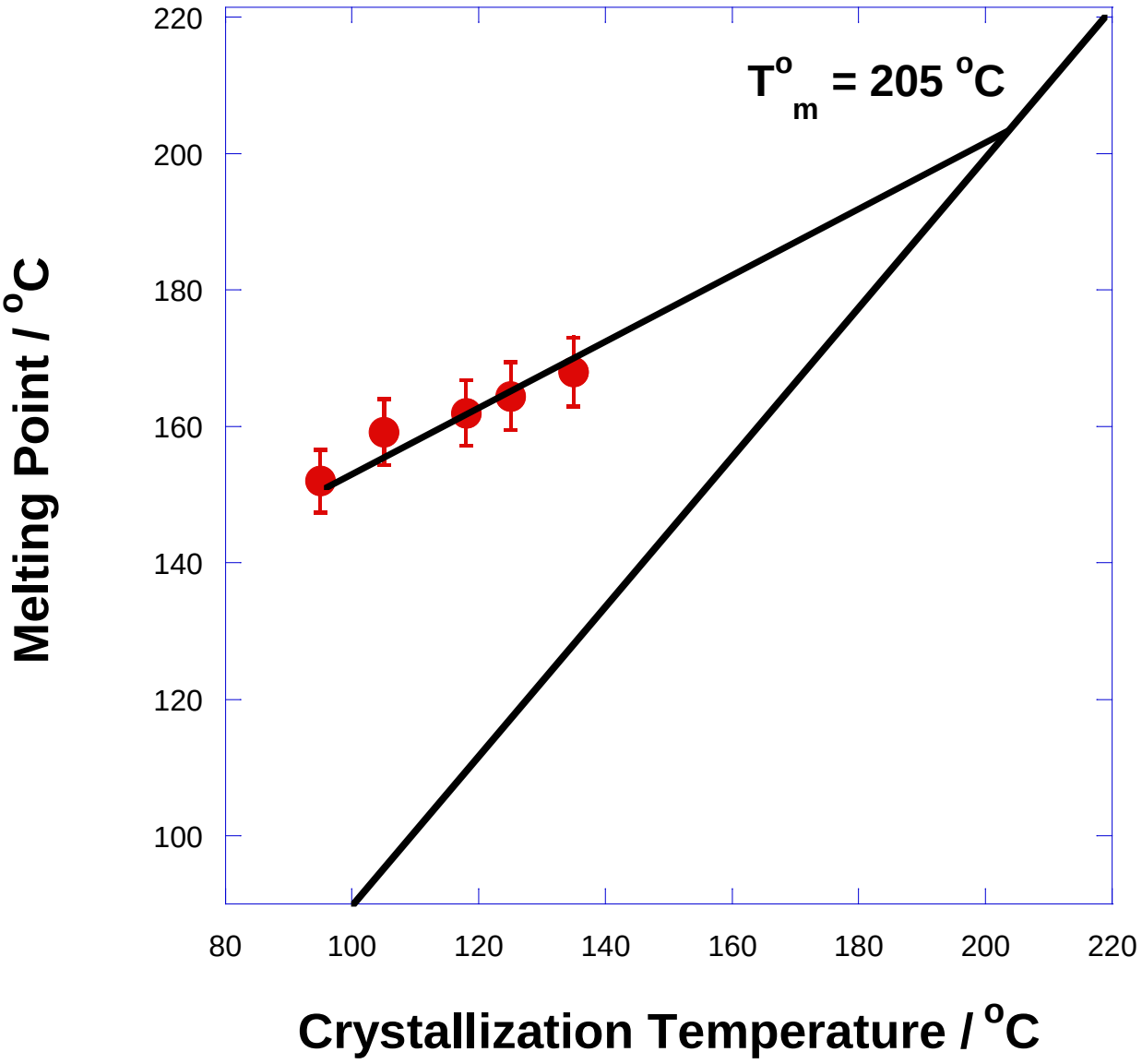

Fig. 8. Hoffman-Weekes plot of T_m against T_c.

The increase in T_m with time at constant temperature is attributed to lamellar thickening and since eq. 5 can be rewritten as

$$\xi = 2\sigma_e / \Delta T.\Delta H_v \qquad (5a).$$

Where ξ is the stem length of the lamellae and $\Delta T = (T^o_m - T_m)$

The thickness was determined at each crystallization temperature and time. It has been repeatedly [8,15,16] shown that lamella thickening develops by growth of the fold surface and this increases with the square root of the lapsed time. The stem length is plotted in Fig. 9 against the square root of the lapsed time and the secondary crystallization rate constant. k_s, listed in Table 1, determined from the slope of the line. The rate constant increased with increasing temperature consistent with it being diffusion rather than nucleation controlled. Diffusion is a thermally activated process and obeys an Arrhenius relationship, such that

$$k_s = A.\exp -\Delta E/ RT \qquad (6).$$

Where A is a pre-exponential factor, R the gas constant and ΔE the activation energy for viscous flow of the chain segments. Fig 10 is the Arrhenius plot for the secondary crystallization rate constant from which the activation energy was 25 ± 5 kJ mol^{-1}. This compares with 40 ± 10 kJ mol^{-1} obtained for poly (ϵ-caprolactone) for the activation energy of viscous flow.

Table 1. Secondary Crystallization Rate Constants.

Crystallization Temperature/ ^oC	95	105	118	125	135
Rate Constant k_s $h^{-1/2}$	0.45	0.48	0.59	0.75	0.90

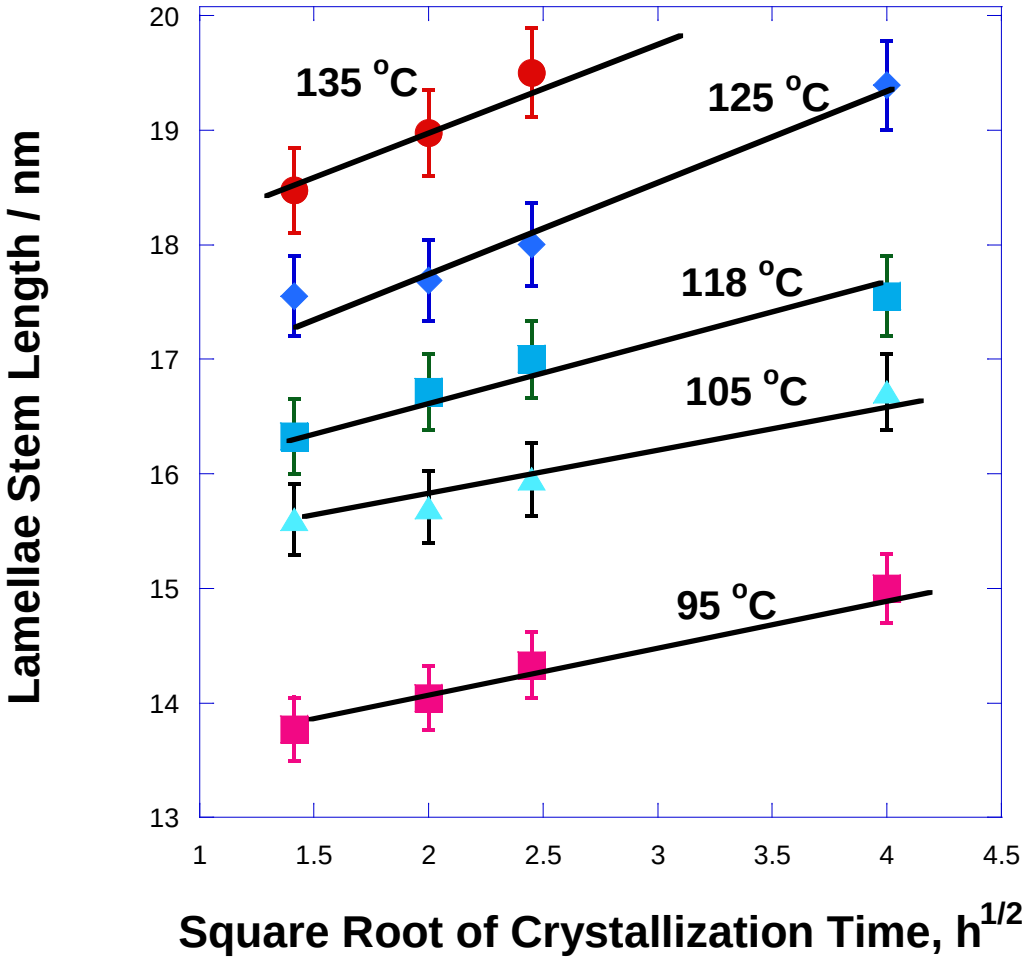

Fig. 9. Dependence of the lamellae stem length on square root of the crystallization time.

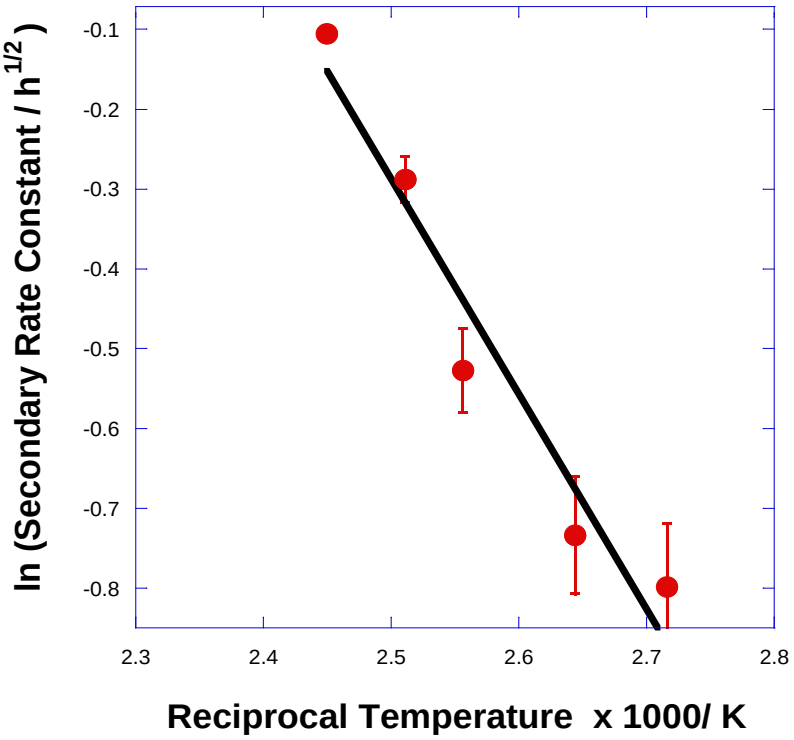

Fig. 10 Arrhenius plot of secondary rate constant.

4.0 Conclusions

Since T_m increases with the time we conclude that the lamellae thicken occurs from the first development of crystallinity and by a process of secondary crystallization in that growth is proportional to the square root of time.

Primary crystallization accounts for the radial growth of the lamellae by secondary nucleation of the growth face, $\alpha\xi$ or $\beta\xi$ in Fig. 11, and the stem length 10-20 nm is determined by the free energy of the fold surface, σ_e, since

$$\xi = 2\sigma_e / \Delta T.\Delta H_v \qquad (5a).$$

Secondary crystallization accounts for the thickening of the lamellae by secondary nucleation of the fold surface, αβ in Fig 11, but since the fold surface does not increased (new top surface area matches the bottom incorporated area) the free energy of the fold surface, σ_e is not involved in the free energy of formation of the critical size nucleus, and by analogy,

$$c = 2\sigma/ \Delta T.\Delta H_v \qquad (5b).$$

Adopting values listed above for σ and σ_e, c must have values between 3 - 6 nm and considerably less than ξ. The free energy of formation of the critical size nucleus for secondary crystallization will also be considerably less than that for primary, making it less rate determining.

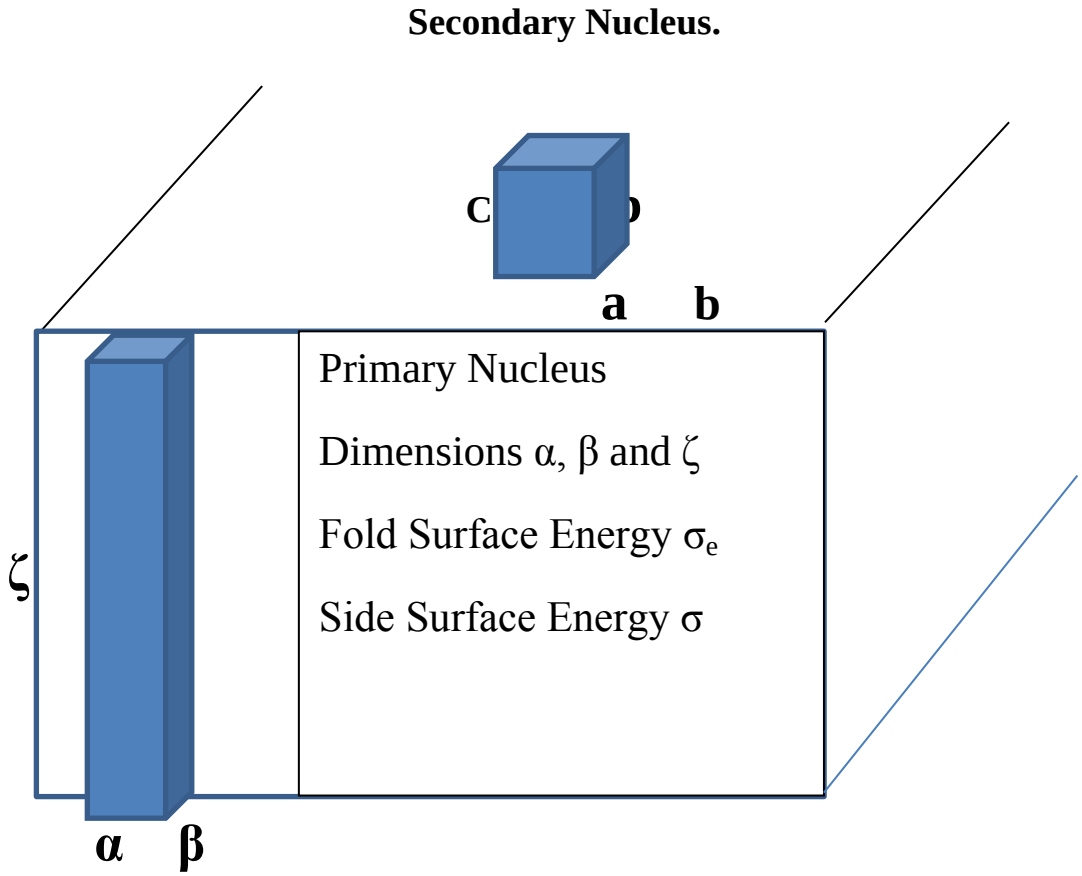

Fig. 11. Schematic Representation of Primary and secondary growth nuclei.

Two time dependent segmental motilities are important in reptation theory [17]; these are linearly dependent on time and on the square root of time. The first involves diffusion over distances greater than between adjacent chain entanglements while the second is less than between chain entanglements where segmental mobility is unhindered by chain

entanglements. The large difference in stem lengths between the two types of secondary nucleation is sufficient to account for the observed time dependences of primary and secondary crystallization.

Acknowledgements

We are indebted To Mr. Frank Biddlestone for technical support.

5 References

[1.] Lu XF, Hay JN, Polymer 2001; **31**: 9423.

[2.] Razavi-Nouri M, Hay JN, J Appl Polym Sci, 2007; **104**:634.

[3.] Blundell DJ, Parker DG, Mehmet-Alkan AA. Hay JN, High Performance Polymers, 1993; **9**:317.

[4.] Feng Y, Jin X, Hay JN, J Appl Polym Sci 1998; **68:**395.

[5.] Feng Y, Jin X, Hay JN, Polymer 1998; **30**:215.

[6.].Vasanthakumari R, Pennings AJ, Polymer 1983; **24: 175.**

[7.] Park JW, Lee JW, Yoo ES, Im ES, Kim SH, Kim YH, Korea Polym J, 1999; **7**: 93.

[8.] Chen Z, Jenkins MJ, Hay JN, Europ Polym J 2014; **50**:225.

[9.] Mills PG, Hay JN, Polymer 1984; **25**: 1277.

[10.] Nicholas P, Lane AR, Carter TJ, Hay JN, Polymer 1988; **29**: 894.

[11.] Jamshidi K, Hyon SH, Ikada Y, Polymer 1988; 29, 2229.

[12.] Garlotta D, J Polym. Environ, 2001; **9**: 63.

[13.] Hoffman JD, Davis GT, Lauritzen JI, in treatise on Solid State Chemistry, volume 3, edited by Hannay NB, Plenum Press, New York 1976.

[14.] Hoffman JD, Weeks JL, J Res Nat Bur Standards 1962; **A73**: 64

[15.] Vasanthakumari R, Pennings AJ, Polymer 1980; **21: 175.**

[16.] Phillipson K, Jenkins MR, Hay JN, J Therm Anal Calorim 2015; **123**; 1491.

[16.] Aziz AA, Samsudin SA, Hay JN, Jenkins MR, Europ Polym J, 2017; **94**: 311.

[17.] Baumingärtner A, Ebert U, Schafer L, J Stat Phys 1998; **90**: 1376.